


Article

Consistent Effects of Canopy vs. Understory Nitrogen Addition on Soil Respiration and Net Ecosystem Production in Moso Bamboo Forests

Chunju Cai ¹, Zhihan Yang ², Liang Liu ², Yunsen Lai ², Junjie Lei ², Shaohui Fan ^{1,*} and Xiaolu Tang ^{3,4,*} 

¹ Key Laboratory of Bamboo and Rattan, International Centre for Bamboo and Rattan, Beijing 100102, China; caicj@icbr.ac.cn

² College of Earth Science, Chengdu University of Technology, Chengdu 610059, China; yangzhihan0526@163.com (Z.Y.); liuliang_cdut@163.com (L.L.); laiyunsen2021@163.com (Y.L.); ljj894180203@163.com (J.L.)

³ College of Ecology and Environment, Chengdu University of Technology, Chengdu 610059, China

⁴ State Environmental Protection Key Laboratory of Synergetic Control and Joint Remediation for Soil & Water Pollution, Chengdu University of Technology, Chengdu 610059, China

* Correspondence: fansh@icbr.ac.cn (S.F.); lxtt2010@163.com (X.T.)

Abstract: Nitrogen (N) deposition has been well documented to cause substantial impacts on ecosystem carbon cycling. However, the majority studies of stimulating N deposition by direct N addition to forest floor have neglected some key ecological processes in forest canopy (e.g., N retention and absorption) and might not fully represent realistic atmospheric N deposition and its effects on ecosystem carbon cycling. In this study, we stimulated both canopy and understory N deposition (50 and 100 kg N ha⁻¹ year⁻¹) with a local atmospheric NH_x:NO_y ratio of 2.08:1, aiming to assess whether canopy and understory N deposition had similar effects on soil respiration (RS) and net ecosystem production (NEP) in Moso bamboo forests. Results showed that RS, soil autotrophic (RA), and heterotrophic respiration (RH) were 2971 ± 597, 1472 ± 579, and 1499 ± 56 g CO₂ m⁻² year⁻¹ for sites without N deposition (CN0), respectively. Canopy and understory N deposition did not significantly affect RS, RA, and RH, and the effects of canopy and understory N deposition on these soil fluxes were similar. NEP was 1940 ± 826 g CO₂ m⁻² year⁻¹ for CN0, which was a carbon sink, indicating that Moso bamboo forest the potential to play an important role alleviating global climate change. Meanwhile, the effects of canopy and understory N deposition on NEP were similar. These findings did not support the previous predictions postulating that understory N deposition would overestimate the effects of N deposition on carbon cycling. However, due to the limitation of short duration of N deposition, an increase in the duration of N deposition manipulation is urgent and essential to enhance our understanding of the role of canopy processes in ecosystem carbon fluxes in the future.

Keywords: canopy nitrogen deposition; understory nitrogen deposition; soil respiration; net primary production; carbon cycling



Citation: Cai, C.; Yang, Z.; Liu, L.; Lai, Y.; Lei, J.; Fan, S.; Tang, X. Consistent Effects of Canopy vs. Understory Nitrogen Addition on Soil Respiration and Net Ecosystem Production in Moso Bamboo Forests. *Forests* **2021**, *12*, 1427. <https://doi.org/10.3390/f12101427>

Received: 1 September 2021

Accepted: 15 October 2021

Published: 19 October 2021

Publisher's Note: MDPI stays neutral with regard to jurisdictional claims in published maps and institutional affiliations.



Copyright: © 2021 by the authors. Licensee MDPI, Basel, Switzerland. This article is an open access article distributed under the terms and conditions of the Creative Commons Attribution (CC BY) license (<https://creativecommons.org/licenses/by/4.0/>).

1. Introduction

Globally, atmospheric nitrogen (N) deposition has increased from two- to three-fold since 1850 due to the increasing atmospheric reactive N emissions derived from combustion, fertilization, and motor vehicles [1–4]. Aside from North America and Europe, China is one of the highest N deposition areas across the globe and has increased by 60% over last three decades [1]. Increased N deposition may lead to a significant impact on carbon cycling in forest ecosystems by changing vegetation growth and soil organic carbon decomposition or accumulation [5–8]. For example, N deposition commonly stimulates primary production and CO₂ sequestration in N-limited forest systems [9]. However, due to strong spatial variability of N deposition and ecosystem N availability [1,10], the effects of N deposition

on carbon cycling varied greatly in forest ecosystems [8,10–12]. Therefore, the size of nitrogen's contribution to the global terrestrial C sink is still debated [9].

Soil respiration (RS), consisting of soil autotrophic respiration (RA) and heterotrophic respiration (RH), is one of the largest carbon fluxes in terrestrial ecosystems. However, estimating RS is of great uncertainty, ranging from 68 to 109 Pg C year^{−1} (1 Pg = 10¹⁵ g) globally, which is about 7–11 times the carbon emission from human activities. Thus, a small change in RS leads to a significant impact on atmospheric CO₂ concentrations. Meanwhile, RH could affect future climate change via the mineralization of long-stored soil carbon, offsetting net primary production (NPP) and even transforming terrestrial ecosystems from a carbon sink to a carbon source [13]. Therefore, an accurate measurement or estimate of RS would greatly improve our understanding of the feedbacks of soil belowground processes to climate change. On the other hand, RS is significantly affected by environmental changes, e.g., N deposition [6,11].

Numerous studies have already evaluated the effects of N deposition on RS; however, these studies yield conflict results showing that N deposition increases [12], decreases [6,11], or does not change RS [14] or leads to different impacts on RS components [11]. The effects of N deposition on RS vary with N deposition rates, N forms, and N ratios [12,15]. For example, results from Li et al. [12] showed that RS with N deposition treatment of 30, 60, and 90 kg N ha^{−1} a^{−1} increased by about 45.7%, 37.7%, and 13.0% compared to that of no N deposition treatment.

Most studies stimulate the effects by applying understory N deposition. However, critical ecological processes, including retention, interception, absorption, and transformation of atmospherically deposited N [16–18], occurring in the forest canopy are usually ignored or assumed to have no effects on the quality and quantity of N deposition on forest soils in understory N deposition [19]. Actually, significant differences in the quality and the quantity of N reaching soil surface are found between the CAN and the UAN experiments due to canopy N retention, interception, absorption, and transformation [18]. As suggested by previous studies [19–21], the traditional understory N deposition stimulating atmospheric N deposition could not fully reflect the actual effects of increasing atmospheric N deposition on forest ecological functions and processes. Therefore, canopy N deposition may overcome these limitations of understory N deposition. Moreover, most of the previous studies used NaNO₃ [22,23], (NH₄)₂SO₄ [23,24], NH₄Cl [25], and NH₄NO₃ [26] as a single N source to stimulating N deposition. However, atmospheric N deposition contains different N forms, e.g., NH_x and NO_y [1]. Different N forms may lead to various impacts on carbon cycling. For example, Du et al. [15] found that inorganic N deposition inhibited RS, while organic N deposition stimulated RS and the ratio of inorganic N and organic N also led to a significant impact on RS in temperate forests. Therefore, stimulating canopy N deposition with different N forms could potentially improve our understanding of actual atmospheric N deposition on carbon cycling in forest ecosystems.

Moso bamboo (*Phyllostachys heterocycla* (Carr.) Mitford *cv. Pubescens*) is one of the most important forest types in subtropical China [27]. Moso bamboo is well known for amazingly rapid growth and can reach a maximum diameter at the breast height (DBH, 13 m) of 8–16 cm and height of 10–20 m within two months after the bamboo shoot emergence [28]. Due to ecological protection, natural forests are not allowed to be felled in China, given that bamboo forest is a major substitute of wood products [29,30]. Thus, the area of Moso bamboo has experienced an increasing trend in recent decades, from 3.87 million hectare during 2004–2008 to 4.68 million hectare during 2014–2018, accounting for more than 70% areas of bamboo forests in China [31,32]. Moreover, Moso bamboo forests contribute a higher net ecosystem production (NEP) compared to other forest types in subtropical China [29,33]. The total NEP of Moso bamboo forests is about 0.027 Pg C year^{−1}, accounting for 15–36% of the NEP of all forests in China [33]; therefore, Moso bamboo forests play a critical role in regional, national, and even global carbon cycling. In recent years, several studies have detected the effects of N deposition on RS in Moso bamboo forests [12,34]. For example, Li et al. [12] found that the N deposition increases RS

and decreases the temperature sensitivity of RS in Moso bamboo forests. However, these studies were conducted via understory N deposition; as indicated above, understory N deposition may not fully reflect the true effects of atmospheric N deposition on RS due to canopy N retention, interception, absorption, and transformation. Moreover, the ratio of N forms was not taken into consideration. Therefore, stimulating canopy N deposition and taking N forms into consideration may potentially improve our understanding of the true effects of atmospheric N deposition on RS and its feedbacks to global climate change in Moso bamboo forests. However, such a study has not been conducted on Moso bamboo forests to the best of our knowledge.

To address this substantial knowledge gap, we conducted a canopy and understory N deposition experiment with a background $\text{NH}_x:\text{NO}_y$ ratio of 2.08:1 in Moso bamboo forests (detailed in method section), aiming to: (1) evaluate the effects on N deposition on RS, RA, and RH; (2) estimate the effects of N deposition on vegetation carbon fluxes and NEP; and (3) compare whether the effects of canopy and understory N deposition on these carbon fluxes were similar. We also hypothesized that understory N deposition overestimated RS, RA, RH, and NEP because of retention, interception, absorption, and transformation of atmospherically deposited N. The outcome of this study may advance our understanding of the true effects of N deposition on RS and NEP in Moso bamboo forests.

2. Materials and Methods

2.1. Study Site

The study was conducted in the National Observation and Research Station of Bamboo Forests of Changning, Sichuan, located at South Sichuan Bamboo Sea which is located in Changning County ($26^\circ 33' 17''$ – $28^\circ 26' 46''$ N, $104^\circ 5' 11''$ – $105^\circ 4' 54''$ E), China. The study area covers an area of 120 km² with a distance of more than 16 km from east to west, and more than 6.5 km from north to south. The station is characterized as a mountainous area with an elevation from 260 to 1000 m [35]. Annual temperature ranges from 14.5 to 18 °C, with the lowest temperature of 8.1 °C in January and highest temperature of 30 °C in summer [35]. The study area has a subtropical humid monsoon climate with annual precipitation of 1200–2000 mm with 334–356 of fog days [35]. The study area is dominated by Moso bamboo (*Phyllostachys edulis*) with about 91% coverage and mixed with few other species, such as *Neosinocalamus affinis* (Rendle) Keng, *Bambusa intermedia* Hsueh et Yi, and *Dendrocalamus membranaceus* Munro [35]. General soil properties are shown in Table 1 that the soil properties in each stand are not significantly different at the level of 0.05 before N deposition.

Table 1. General soil properties in Moso bamboo forests (mean \pm standard deviation).

Treatment	pH	TN (g kg ^{−1})	AN (mg kg ^{−1})	SOM (g kg ^{−1})	TK (g kg ^{−1})	AK (mg kg ^{−1})	TP (mg kg ^{−1})	AP (mg kg ^{−1})
CN100	4.00 \pm 0.35 a	2.21 \pm 0.47 a	221.24 \pm 36.38 a	63.98 \pm 11.82 a	9.48 \pm 1.36 a	39.87 \pm 5.52 a	306.52 \pm 32.10 a	0.47 \pm 0.17 a
CN50	3.87 \pm 0.15 a	2.82 \pm 0.45 a	271.51 \pm 60.28 a	75.26 \pm 16.40 a	11.32 \pm 3.5 a	47.00 \pm 4.73 a	376.30 \pm 22.60 a	1.44 \pm 1.18 a
CNP0	3.97 \pm 0.06 a	1.97 \pm 0.09 a	223.52 \pm 38.00 a	52.33 \pm 2.23 a	10.61 \pm 1.86 a	39.77 \pm 4.24 a	288.48 \pm 41.66 a	0.47 \pm 0.11 a
GN100	4.00 \pm 0.20 a	1.86 \pm 0.46 a	186.49 \pm 34.94 a	54.15 \pm 16.48 a	8.48 \pm 1.23 a	35.66 \pm 2.29 a	276.27 \pm 30.99 a	0.91 \pm 0.53 a
GN50	4.00 \pm 0.17 a	2.02 \pm 0.57 a	221.65 \pm 64.05 a	55.55 \pm 19.07 a	12.15 \pm 1.98 a	42.15 \pm 10.50 a	305.60 \pm 55.65 a	0.52 \pm 0.19 a

Note: the same letter after the numbers indicates no significant difference at $p = 0.05$ among different nitrogen deposition treatments analyzed by one-way analysis of variance. CN0: canopy water addition without any N addition; CN50 and CN100: canopy N deposition with 50 and 100 kg N ha^{−1} year^{−1}, respectively; GN50 and GN100: understory N deposition with 50 and 100 kg N ha^{−1} year^{−1} (GN100), respectively. TN: total nitrogen content (g kg^{−1}); AN: available nitrogen content (mg kg^{−1}); SOM: soil organic matter (g kg^{−1}); TK: total potassium content (g kg^{−1}); AK: available potassium content (mg kg^{−1}); TP: total phosphorus content (mg kg^{−1}); and AP: available phosphorus content (mg kg^{−1}).

2.2. Study Design

A randomized block design was applied for this study in March 2019. Each block with three replicates contained five (5 m radius) circle plots to which the five treatments were randomly assigned: control–canopy water addition without any N addition (CN0); canopy N deposition with 50 kg N ha^{−1} year^{−1} (CN50); canopy N deposition with 100 kg N ha^{−1} year^{−1} (CN100); understory N deposition with 50 kg N ha^{−1} year^{−1} (GN50); and

understory N deposition with $100 \text{ kg N ha}^{-1} \text{ year}^{-1}$ (GN100) with a local ratio of NH_x and NO_y was 2.08:1 of our study area according to Tian et al. [36]. A buffer zone of 5–10 m was set between two nearly plots.

N deposition experiment was conducted in the middle of each month from April to September during 2019–2021. Specifically, ammonium salt ($\text{NH}_4\text{-N}^+$) was the source of (NH_x), and nitrate ($\text{NO}_3\text{-N}^-$) was the source of NO_y . In each N deposition plot, a mixed solution of NH_x and NO_y was added in a volume equivalent of 1 mm of precipitation and amounted to 6 mm per year (six times per year). This amount equaled less than 0.5% of annual precipitation; thus, the confounding impacts caused by water addition was negligible. Canopy N deposition was applied using an irrigation system with a forest canopy spraying system built in the plot center and pumped to a height that was about two meters above forest canopy. The N solutions were evenly sprayed onto the canopies by a sprinkler that could freely turn 360° . To minimize the effect of sunshine and wind speed, sprays were conducted in the morning. The first N deposition treatment was conducted in the middle of April 2019. To partition RA and RH, a $100 \text{ cm} \times 100 \text{ cm}$ subplot was trenched to a depth of 80 cm in the plot center in March 2019. Vegetation and litter in the subplots were removed carefully to minimize soil disturbance, and the subplots were kept free of live vegetation and litter throughout the study period [37]. Since the majority of roots of Moso bamboo were distributed within 40 cm of the surface (Tang et al., 2012), a trench of 80 cm was sufficient to achieve the objectives of this study. Four 0.5 cm thick polyethylene boards were inserted into the trenches vertically to prevent root ingrowth after trenching. In each plot, three sampling polyvinyl chloride collars (PVC, 20 cm inside diameter \times 12 cm height, two for untrenched soil and one for trenched soil) were inserted into the soil at a depth of 6 cm. Once the collars were installed in the soil, they remained there throughout the study period. Subsequently, the soil carbon fluxes in the trenched plot represent RH, which represents the carbon flux from the decomposition of litter detritus and soil organic matter by microorganisms [38]. Consequently, RA was calculated as the difference between RS and RH [29,39].

2.3. RS Measurement

Four months after trenching, RS measurement began in July 2019 and lasted for two years until June 2021 using a Li-Cor-8100 (Li-Cor Inc., Lincoln, NE, USA) automated soil CO_2 flux system. Soil CO_2 flux measurement was conducted between 9:00 and 12:00 a.m., since RS in this period could represent the diurnal average [37,39,40]. Soil temperature (ST, $^\circ\text{C}$) and moisture (SM, %) near the collars at the depth of 5 cm were also measured while measuring CO_2 flux over the entire study period.

2.4. Bamboo, Root, and Litterfall Production

DBH of all bamboos in each subplot were measured using a diameter tap in each July during the study period. Age of each individually bamboo was recorded based on visual examination of the culm color, eyelash on cycle of culm sheath, powder under cycle of culm sheath, and sheath in culm base [29,41]. Biomass of individual bamboos was estimated as [42]:

$$\text{Biomass} = 747.784 \times \text{DBH}^{2.771} \times [(0.148 \times A)/(0.028 + A)]^{5.555} + 3.772 \quad (1)$$

where A is age (du) [42] and DBH is diameter at breast height (1.3 m). Annual NPP of bamboo was calculated as the sum of the biomass of the growth increment of newly established (1 “du”), 2, 3, and 4 “du” bamboos. A carbon content of 0.5 was used to convert biomass to carbon [43].

Following Tang et al. [44], root production was calculated by a maximum–minimum approach [45,46]. Specifically, bamboo roots were collected by sequential soil cores (5 cm in diameter) every two months from July 2019 to June 2020. Five soil cores were randomly selected in each plot for three soil layers: 0–10, 10–30, and 30–50 cm because the majority of bamboo roots were distributed within 0–40 cm [47]. Finally, a total of 900 soil sequential

cores were collected. After root collection, roots were manually washed to remove soils. In the laboratory, root samples were dried to a constant weight at 65 °C and weighed to the nearest 0.01 g. Similarly, a carbon content of 0.5 was used to convert root biomass to carbon [43].

Monthly litterfall was collected using three 1 m × 1 m collectors within each plot. The collectors were located at angles of 0°, 120°, and 240° at three meters from plot center. All litterfall were dried to a constant weight at 65 °C, and a carbon content of 0.5 was used to convert biomass to carbon [43].

2.5. Data Analysis

All data analysis was performed in R 3.6.2 [48]. One-way analysis of variance (ANOVA) was conducted to compare the difference of carbon flux components among different N deposition treatments at the level of 0.05. Two-way analysis of variance was conducted to evaluate the effects of month, N deposition treatment, and their interactions on different carbon flux components. A linear regression analysis was applied to determine the relationships between RS, or RA or RH and SM. The widely used exponential regression model was performed to analyze the relationships between RS, or RA or RH and ST as follows [49]:

$$RS \text{ (RA or RH)} = a \times e^{b \times ST} \quad (2)$$

where RS, RA, and RH are the average total soil respiration, autotrophic, and heterotrophic respiration rate in each plot ($\mu\text{mol CO}_2 \text{ m}^{-2} \text{ s}^{-1}$). ST (°C) is the measured soil temperature at 5 cm depth, and a and b are the coefficients.

The Q_{10} value, which is the respiration rate increase as temperature increases by 10 °C, was applied to explain the sensitivity of respiration to soil temperature. For each treatment, the Q_{10} value was calculated based on monthly RS and soil temperature in each plot. Q_{10} values were calculated with the following formula [50]:

$$Q_{10} = (a \times e^{b \times (ST+10)}) / (a \times e^{b \times ST}) = e^{10b} \quad (3)$$

where b is taken from Formula (2).

The accumulative CO_2 emission was calculated by:

$$F(R) = \sum_{i=1}^{12} R_i \times 10^{-6} \times 44 \times 10^4 \times 3600 \times 24 \times \text{days} \quad (4)$$

where $F(R)$ is the accumulative CO_2 emission ($\text{g CO}_2 \text{ m}^{-2} \text{ year}^{-1}$), R_i is the average monthly respiration rate ($\mu\text{mol CO}_2 \text{ m}^{-2} \text{ s}^{-1}$) of RS, or RA or RH; “days” is the number of days in each month; the 10^{-6} is the unit conversion of 1 μmol to 1 mol. Due to COVID-19, soil fluxes in February, March, and December 2020 were not measured. Therefore, when calculating annual RS, RA, and RH, we used soil fluxes in February and March 2021 and December 2019 instead.

In forest ecosystems, NEP can be calculated as the balance between NPP of vegetation and RH [29,51]:

$$NEP = NPP - RH \quad (5)$$

where NPP is the net primary production ($\text{g CO}_2 \text{ m}^{-2} \text{ year}^{-1}$), which is the sum of the annual vegetation NPP (both aboveground and belowground) and litterfall; RH is the annual carbon flux from heterotrophic respiration ($\text{g CO}_2 \text{ m}^{-2} \text{ year}^{-1}$), respectively.

3. Results

3.1. Seasonal Variations of ST and SM

Regardless of N deposition, ST and SM at 5 cm depth in trenched (Figure 1a,c) and untrenched (Figure 1b,d) showed pronounced seasonal variability (Figure 1 and Table 2). ST ranged from 2.5 °C in January to 28.7 °C in August with an annual average ST of 18.0 °C for untrenched plots and 18.1 °C for trenched subplots (Figure 1a,b). No significant

difference was observed between untrenched and trenched plots for different N deposition treatments (Table S1, $p > 0.694$). ST was not significantly affected by N deposition in both trenched ($p = 0.089$) and untrenched plots ($p = 0.376$). Month had a significant impact on ST ($p < 0.001$), while the interactions of N deposition and month did not affect ST.

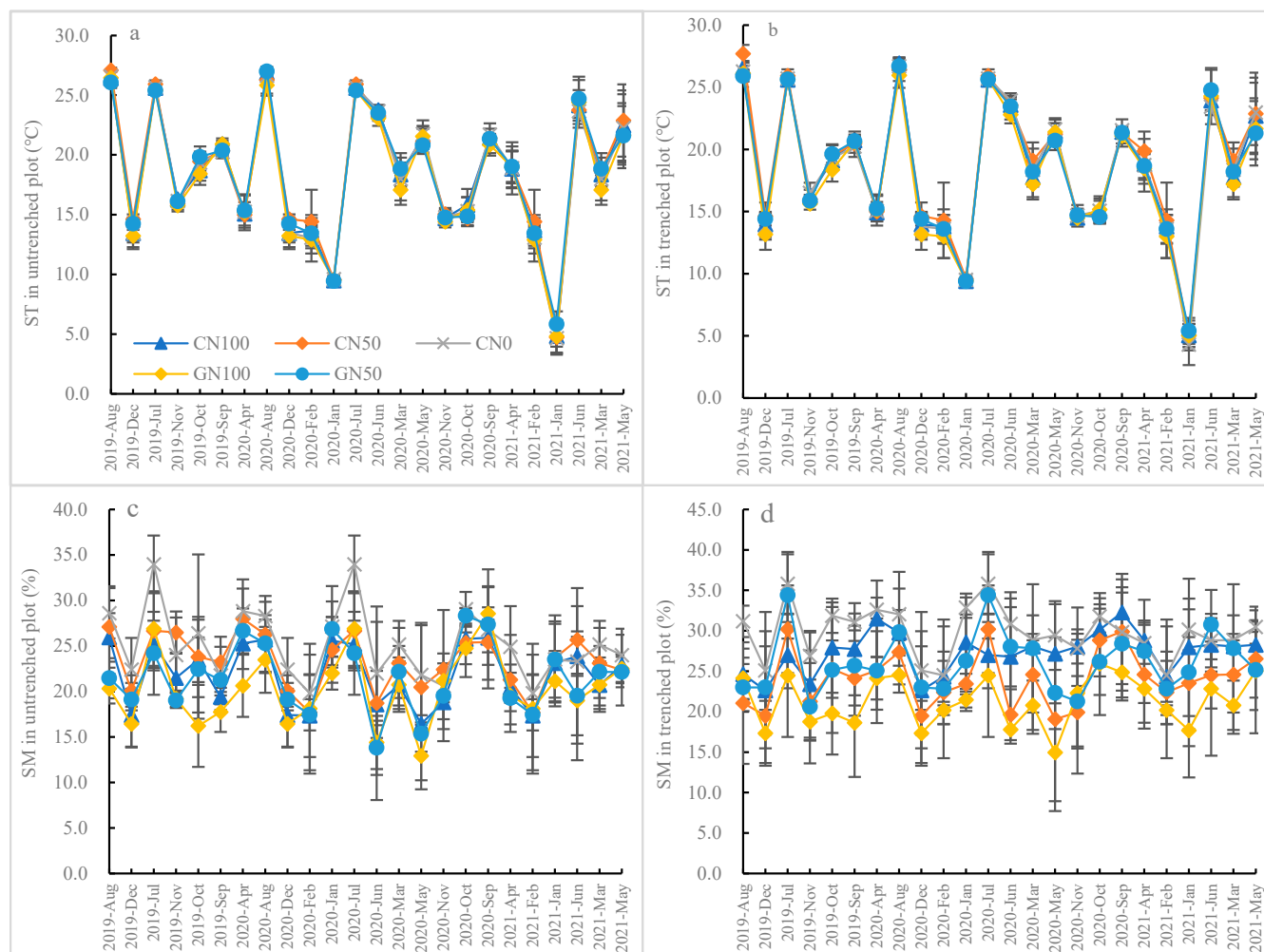


Figure 1. Seasonal variations of soil temperature (ST, °C) and moisture (SM, %). (a) ST at 5 cm depth in trenched plots, (b) ST at 5 cm depth in untrenched plots, (c) SM at 5 cm depth in trenched plots, (d) SM at 5 cm depth in untrenched plots. CN0: canopy water addition without any N addition; CN50 and CN100: canopy N deposition with 50 and 100 kg N ha⁻¹ year⁻¹, respectively; GN50 and GN100: understory N deposition with 50 and 100 kg N ha⁻¹ year⁻¹ (GN100), respectively.

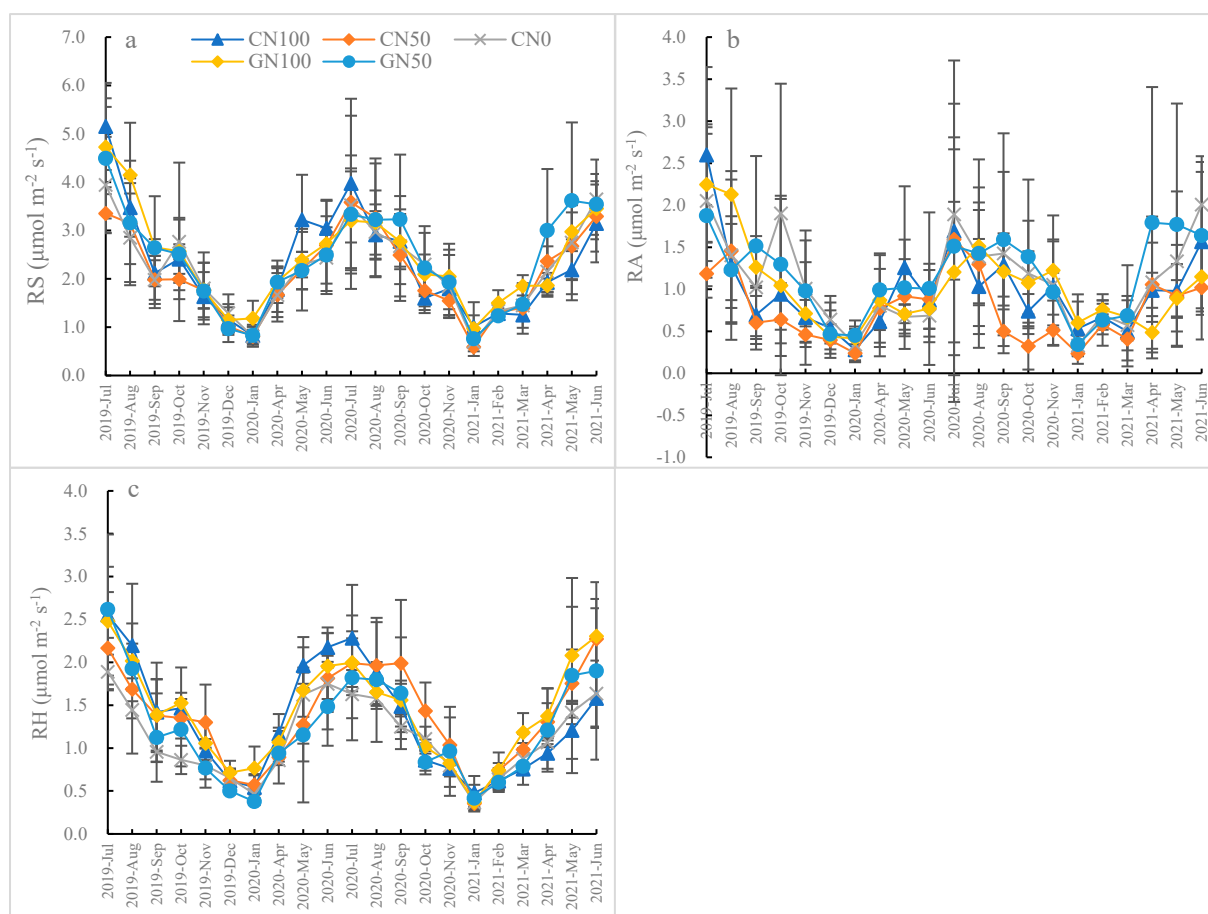
Similarly, seasonal variability was also observed in SM (Figure 1c,d), and month significantly affected SM ($p < 0.011$, Table 2) in both trenched and untrenched plots. SM changed from 8.6% to 39.9% with an annual mean SM of 22.4% from untrenched plots and 25.1% for trenched subplots. N deposition significantly affected SM in both trenched ($p < 0.001$, Table 2) and untrenched plots ($p = 0.008$); however, SM was not affected by the interactions of N deposition and month.

Table 2. *p* values of two-way analysis of the interactions of N addition and month on soil temperature (ST), soil moisture (SM), total soil respiration (RS), autotrophic respiration (RA), and heterotrophic respiration (RH).

Treatment	ST		SM		RS	RA	RH
	Trenched	Untrenched	Trenched	Untrenched			
N deposition	0.089	0.376	<0.001	0.008	0.128	0.009	<0.001
Month	<0.001	<0.001	<0.001	0.011	<0.001	<0.001	<0.001
N deposition × month	1	1	1	0.831	0.999	1	0.808

3.2. Seasonal Variations of Respiration Rates

There were seasonal variations in RS, RA, and RH, with the highest respiration rate in each July and the lowest in each January (Figure 2). RS was not affected by N deposition ($p = 0.128$, Table 2). Mean annual RS was for $2.25 \pm 0.89 \mu\text{mol m}^{-2} \text{s}^{-1}$ for CN0, and it was 2.14 ± 0.88 , 2.32 ± 1.09 , 2.40 ± 1.02 , and $2.43 \pm 0.97 \mu\text{mol m}^{-2} \text{s}^{-1}$ for CN50, CN100, GN50, and GN100, respectively (Figure 2). RS under canopy and understory N deposition was not significantly different ($p > 0.05$).

**Figure 2.** Monthly variability of total soil respiration (RS, (a)), autotrophic respiration (RA, (b)), and heterotrophic respiration (RH, (c)) ($\mu\text{mol CO}_2 \text{m}^{-2} \text{s}^{-1}$) from July 2019 to June 2021. CN0: canopy water addition without any N addition; CN50 and CN100: canopy N deposition with 50 and 100 kg N ha^{−1} year^{−1}, respectively; GN50 and GN100: understory N deposition with 50 and 100 kg N ha^{−1} year^{−1} (GN100), respectively.

Mean annual RA was $1.12 \pm 0.53 \mu\text{mol m}^{-2} \text{s}^{-1}$ for CN0, which was similar to RA under GN50 treatment. Although mean RA rate under CN0 was 47% higher than that of under CN50 treatment and 13% and 10% higher than that of CN100 and GN100 treatments,

the differences were not significant. N deposition significantly affected RA rate ($p = 0.009$, Table 2), and the interactions of N deposition and month did not significantly affect RA.

Mean annual RH was $1.13 \pm 0.45 \mu\text{mol m}^{-2} \text{s}^{-1}$ for CN0, which was 22%, 18%, 9%, and 26% lower than RH under CN50, CN100, GN50, and GN100 treatments, respectively. RH rate was significantly affected by N deposition ($p < 0.001$, Table 2); however, the interactions of N deposition and month did not significantly affect RH ($p = 0.808$). RH rates under canopy and understory N deposition did not differ significantly ($p > 0.05$).

RS, RA, and RH rates were exponentially correlated with ST regardless of N deposition levels. ST could explain 52–74% variations of RS, 20–45% for RA, and 52–76% for RH (Figure 3 and Table 3). Calculated Q_{10} values of RS, RA and RH were 1.81, 1.71, and 1.90 for CN0; 1.96, 2.43, and 1.77 for CN50; 1.96, 1.76, and 2.12 for CN100; 1.82, 1.64, and 2.02 for GN50; and 1.81, 1.62, and 1.94 for GN100, respectively (Table 3). However, there was no significant correlation between RS, RA, RH, and SM (Table S2 and Figure S1).

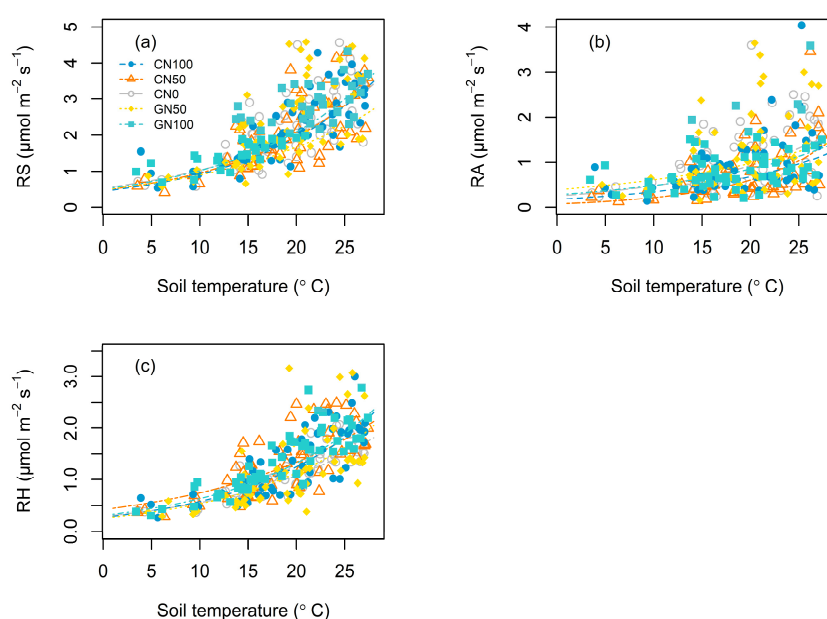


Figure 3. The correlations between total soil respiration (RS, (a)), autotrophic respiration (RA, (b)), heterotrophic respiration (RH, (c)), and soil temperature ($^{\circ}\text{C}$) at 5 cm under nitrogen deposition. CN0: canopy water addition without any N addition; CN50 and CN100: canopy N deposition with 50 and 100 $\text{kg N ha}^{-1} \text{year}^{-1}$, respectively; GN50 and GN100: understory N deposition with 50 and 100 $\text{kg N ha}^{-1} \text{year}^{-1}$ (GN100), respectively.

Table 3. Coefficients of different models of the relationships between soil respiration ($\mu\text{mol CO}_2 \text{m}^{-2} \text{s}^{-1}$) and soil temperature ($^{\circ}\text{C}$) at 5 cm depth.

Model	Coefficients	RS					RA					RH				
		CN100	CN50	CN0	GN50	GN100	CN100	CN50	CN0	GN50	GN100	CN100	CN50	CN0	GN50	GN100
$\text{RS (RA or RH)} = a \times e^{b \times \text{ST}}$	a	0.580	0.554	0.685	0.723	0.739	0.303	0.125	0.375	0.437	0.379	0.287	0.438	0.312	0.296	0.381
	b	0.067	0.067	0.059	0.060	0.060	0.056	0.089	0.054	0.050	0.049	0.075	0.057	0.064	0.070	0.066
	R^2	0.718	0.547	0.592	0.519	0.735	0.446	0.317	0.302	0.202	0.336	0.713	0.543	0.771	0.515	0.764
Q_{10}		1.96	1.96	1.81	1.82	1.81	1.76	2.43	1.72	1.64	1.62	2.12	1.77	1.90	2.02	1.94

3.3. Total Annual CO_2 Fluxes from RS

Regardless of N deposition amount, N deposition did not significant affect the cumulative CO_2 fluxes of RS, RA, and RH, and the cumulative CO_2 fluxes of RS, RA, and RH among canopy and understory N deposition were not significantly different (Table 4). RS was $2971 \pm 597 \text{ g CO}_2 \text{m}^{-2} \text{year}^{-1}$ for CN0, and it was 2817 ± 563 , 3039 ± 324 , 3141 ± 854 , and $3227 \pm 356 \text{ g CO}_2 \text{m}^{-2} \text{year}^{-1}$ for CN50, CN100, GN50, and GN100, respectively (Table 4). RA contributed 50% of RS for CN0, 43% for CN100, 36% for CN50, 42% for GN50, and 49% for GN100. The contribution of RH to RS was higher than that of RA, and RH

contributed 50%, 64%, 57%, 58%, and 54% of RS for CN100, CN50, CN100, GN50, and GN100, respectively.

Table 4. Annual carbon fluxes ($\text{g CO}_2 \text{ m}^{-2} \text{ year}^{-1}$) from July 2019 to June 2021 among different nitrogen addition treatments.

Treatment	RS	RA	RH	NPP	Litterfall	Root NPP	NEP
CN100	3039 \pm 324 a	1303 \pm 422 a	1737 \pm 282 a	1581 \pm 362 a	1594 \pm 545 a	915 \pm 367 a	1439 \pm 440 a
CN50	2817 \pm 563 a	1008 \pm 361 a	1810 \pm 340 a	1067 \pm 493 a	1498 \pm 354 a	907 \pm 302 a	755 \pm 654 a
CN0	2971 \pm 597 a	1472 \pm 579 a	1499 \pm 56 a	1742 \pm 399 a	1696 \pm 509 a	705 \pm 149 a	1940 \pm 826 a
GN100	3227 \pm 356 a	1348 \pm 476 a	1880 \pm 186 a	1336 \pm 1092 a	1756 \pm 595 a	716 \pm 205 a	1212 \pm 1249 a
GN50	3141 \pm 854 a	1527 \pm 887 a	1614 \pm 532 a	1685 \pm 502 a	1744 \pm 922 a	724 \pm 134 a	1815 \pm 831 a

Note: the same letter after the number indicates no significant difference at $p = 0.05$ among different nitrogen addition treatments analyzed by one-way analysis of variance.

N deposition did not significantly affect vegetation NPP and litterfall production (Table 4). Specifically, NPP was $1742 \pm 399 \text{ g CO}_2 \text{ m}^{-2} \text{ year}^{-1}$ for CN0, which was higher than NPP for CN50, CN100, GN50, and GN100; however, the difference was not significant ($p = 0.342$). Although litterfall production was $1696 \pm 509 \text{ g CO}_2 \text{ m}^{-2} \text{ year}^{-1}$ under CN0 treatment and it was higher than that of canopy N deposition (CN100 and CN50) and lower than understory N deposition (GN50 and GN100), litterfall production among different N deposition treatments was not significantly different ($p = 0.941$). Root NPP was $705 \pm 149 \text{ g CO}_2 \text{ m}^{-2} \text{ year}^{-1}$ for CN0, and it did not differ significantly among different N deposition treatment ($p = 0.365$).

Similarly, canopy and understory N deposition did not significantly affect NEP ($p = 0.138$). NEP was $1940 \pm 826 \text{ g CO}_2 \text{ m}^{-2} \text{ year}^{-1}$ for CN0, and it was 755 ± 654 for CN50, 1439 ± 440 for CN100, 1815 ± 831 for GN50, and $1212 \pm 1249 \text{ g CO}_2 \text{ m}^{-2} \text{ year}^{-1}$ for GN100.

4. Discussion

4.1. RS and NEP in Moso Bamboo Forests

In this study, annual cumulative CO_2 fluxes of RS without N deposition was $2971 \pm 597 \text{ g CO}_2 \text{ m}^{-2} \text{ year}^{-1}$, which was lower than that of Moso bamboo forest in Hunan province ($3390 \text{ g CO}_2 \text{ ha}^{-1} \text{ year}^{-1}$) [52], Tianmu Mountain ($5290 \text{ g CO}_2 \text{ ha}^{-1} \text{ year}^{-1}$) [53], Qingshan town ($5680 \text{ g CO}_2 \text{ ha}^{-1} \text{ year}^{-1}$) [54], and the Wanhuling Natural Reserve in Fujiang Province ($4990 \text{ g CO}_2 \text{ ha}^{-1} \text{ year}^{-1}$) [55]. Liu et al. [54] and Wang et al. [56] attributed this variability to climate conditions, such as temperature and precipitation, and different measurement approaches of soil CO_2 fluxes. For example, mean annual temperature in the study area of Wanhuling Natural Reserve in Fujiang Province was 19.4°C , which was higher than that in our study area, and respiration rates were exponentially related with temperature (Figure 3) and [55]. However, annual cumulative CO_2 fluxes of RS under CN0 treatment was higher than that of subtropical bitter bamboo (*Pleuroblastus amarus*, $1569 \text{ g CO}_2 \text{ m}^{-2} \text{ year}^{-1}$) close to our study area [57]. This difference may be attributed to different bamboo species. Bitter bamboo was a small bamboo type with relatively lower production compared to Moso bamboo forests. NPP (aboveground + belowground + litterfall) was $4963 \text{ g CO}_2 \text{ m}^{-2} \text{ year}^{-1}$ in our study, which was 24% higher than that of bitter bamboo [57].

Q_{10} values of RS at the soil depth of 5 cm was 1.81, which was slightly higher than that of RA and lower than 1.90, indicating RH was more sensitive to temperature. Our results were similar to Tang et al. [29], who found that Q_{10} was 1.9 for RS, 1.8 for RA, and 2.0 for RH. However, our results were lower than that in deciduous broadleaf (2.45) and needle-leaved forests (3.26) across temperate China, and in evergreen broadleaf (2.38) and needle-leaved forests (2.38) at 5 cm depth across subtropical China [58]. These results demonstrated that RS was less sensitive to increasing temperature and thus smaller priming effects on soil CO_2 fluxes in Moso bamboo forests compared to temperate and subtropical forests in China.

RA contributed 36–50% to RS, and RH contributed 50–58% to RS regardless of N deposition levels, which followed the reported range in previous studies [59]. Although our study showed the ratio of RH/RS was not significantly higher, the ratio of RH/RS increased regardless of canopy or understory N deposition or N levels. This result had important implications for understanding soil carbon cycling. Because one of the important sources of RH was from the decomposition of soil organic matter due to microbial activities [60], the increased ratio of RH/RS potentially led to more soil carbon loss under ongoing N deposition. Based on a global dataset, Bond-Lamberty et al. [61] found a rising RH/RS ratio from 1990 to 2014 and attributed such increase in RH/RS ratio to the elevated temperature under global climate change. Our finding could propose another potential mechanism that the increasing RH/RS ratio may also be caused by increasing N deposition in the last several decades.

NEP is a key parameter to evaluate the capability of carbon sequestration at an ecosystem scale in terrestrial ecosystems. NEP was $1940 \pm 826 \text{ g CO}_2 \text{ m}^{-2} \text{ year}^{-1}$ under CN0, which was higher than that of a *Castanopsis kawakamii* forest in subtropical China ($1500 \text{ g CO}_2 \text{ m}^{-2} \text{ a}^{-1}$) [62], an Asian tropical rain forest ($3.59\text{--}8.62 \text{ g CO}_2 \text{ m}^{-2} \text{ year}^{-1}$) [63], the average of main forest types in China, e.g., boreal forests ($495 \text{ g CO}_2 \text{ m}^{-2} \text{ year}^{-1}$), temperate forests ($1382 \text{ g CO}_2 \text{ m}^{-2} \text{ year}^{-1}$), subtropical forests ($1800 \text{ g CO}_2 \text{ m}^{-2} \text{ year}^{-1}$), and tropical forests ($983 \text{ g CO}_2 \text{ m}^{-2} \text{ year}^{-1}$) [64], and the average magnitude of global forests ($865 \text{ g CO}_2 \text{ m}^{-2} \text{ year}^{-1}$) [65]. These differences may be attributed to tree species and their biological characteristics, soil and climate conditions, and different method applications [66,67]. These results further indicate that Moso bamboo is a more productive forest type that can sequester more carbon per unit area from the atmosphere compared with other forest types, playing an important role in alleviating global climate change [33].

4.2. Effects of N Deposition on Carbon Flux Components

Based on the two-year experiment of N deposition, we compared the effects of canopy and understory N deposition on RS, its components, and NEP, and further examined the changes of these carbon fluxes differed from canopy and understory N deposition. Although the effects of canopy N deposition on carbon cycling have been evaluated in several different forest types [18,68], to our best knowledge, this study was the first time to assess whether the changes of RS, its components, and NEP caused by canopy and understory N deposition differed in Moso bamboo forests using a similar ratio of atmospheric N forms ($\text{NH}_x:\text{NO}_y = 2.08:1$), which could more accurately represent realistic N deposition in forest ecosystems. However, contrary to our initial hypothesis and to the suggestion from Zhang et al. [19], canopy and understory N deposition had similar effects on soil and vegetation carbon fluxes. The observed consistent effects of canopy and understory N deposition on RS and NEP may be attributed to several reasons.

First, the most direct reason may be that few or no N were retained, intercepted, or absorbed by the bamboo canopy in which the quantity of N reaching the soil was similar between canopy and understory N deposition. We lacked direct evidence for such explanation because the factors that were likely to remove N through canopy to soil were absent, e.g., wind and precipitation. However, studies from recent decades of different forest types have clearly demonstrated that forest canopy retains a substantial proportion of deposited atmospheric N in forms of N retention, absorption, and uptake [16–18,69]. On the other hand, Moso bamboo forest is a special forest type with many different characteristics compared to other forest types, such as fast growing, smooth barks that find it difficult to absorb N. However, there was no such study to quantify the canopy retention and absorption of deposited N in Moso bamboo forests.

Second, canopy N retention ability may be saturated because of extremely high background of N deposition of ranging from 82 to $113 \text{ kg N ha}^{-1} \text{ year}^{-1}$ [70], which was much higher than average N deposition of $20.4 \text{ kg N ha}^{-1} \text{ year}^{-1}$ across China [1]. With the saturation of N retention capability, the experimental N deposition would be not retained and absorbed, which could directly pass through the canopy to forest floor.

Third, despite the amount of N reaching soil being reduced by forest canopy, soil properties that affect RS may be relatively stable and insensitive to N addition because natural N deposition was high enough. As we indicated above, natural N deposition was up to $113 \text{ kg N ha}^{-1} \text{ year}^{-1}$ in the study area [70]—such that the effects of experimental N addition on soil properties reached a stable level. Therefore, the responses of RS and its components to canopy and understory N deposition were similar. Such a phenomenon has been observed in a mixed forest in subtropical China that soil properties, including soil exchangeable cations and microbial communities, were not different between canopy and understory N deposition [71].

Finally, the short duration of N deposition experiment may be another reason for the consistent effects of canopy and understory N deposition on vegetation fluxes in current study. We expected that canopy N deposition had different effects on vegetation fluxes because of N absorption in canopy. Such effects could change the vegetation physiology [8,72]. This effect, however, needed time [73]; perhaps, it was more than two years for Moso bamboo forests. Therefore, within such a short experimental duration, it is hard to distinguish the effects of canopy and understory N deposition on vegetation and soil carbon fluxes in Moso bamboo forests.

4.3. Uncertainties

Although this study was the first attempt to compare the effects of canopy and understory N deposition on RS and NEP, uncertainties still exist in a few aspects. First, the trenching approach may be a potential factor that affects RH due to the remaining roots and associated root exudates [59], which are respired by soil microbes and raise a priming effect on the microbial breakdown of SOC [74]. To reduce such uncertainty, we set the trench plot four months before soil flux measurement. A previous study also proposed that elevated SM in trenched plot could increase RH [29]. However, the increased SM may be not an impact factor for RH in the current study because there was not a significant correlation between SM and RH (Figure S1 and Table S2). Second, it should be noted that due to methodological limitations, RA estimated from trenching approach included not only root respiration (source from root growth and maintenance respiration) but also rhizosphere respiration (mycorrhizal respiration and rhizospheric priming effects) [75]. Mycorrhizal respiration is not strictly autotrophic respiration as it is regulated by mycorrhizal fungi. Third, N deposition lasted for two years in currently study. Previous studies have found that the duration of N deposition led to a significant impact on RA and RH [11,76], and the dominant factor varied with N deposition duration [11]. Therefore, canopy N deposition with a longer duration would further improve our understanding of the interactions between N deposition and forest canopies and their effects on carbon cycling in Moso bamboo forests. In addition, our study was a case study, which had different a stand, site, and climate conditions compared to other studies; therefore, similar studies among different forest types in varying site and climate conditions are encouraged in future.

5. Conclusions

In this study, we distinguished the effects of canopy and understory N deposition on RS and NEP in Moso bamboo forests in subtropical China. We found that NEP was $1940 \pm 826 \text{ g CO}_2 \text{ m}^{-2} \text{ year}^{-1}$, which was higher than that of the majority forest types across China, indicating that Moso bamboo forests are playing an important role in alleviating global climate change. However, RS, its component, and NEP were not affected by N deposition, and the effects of canopy and understory N deposition on RS and NEP were similar. These findings did not support our hypothesis and prediction from other studies Zhang et al. [19], who expected that understory N deposition underestimated RS and NEP because of retention, interception, absorption, and transformation of atmospherically deposited N. Nonetheless, whether ecosystem carbon fluxes respond differently to canopy and understory N deposition needs longer duration of field observations; thus, a relative short-time two-year N deposition manipulation could be a main limitation in this study.

Given the importance of N deposition in forest canopy processes and the lack of direct evidence in Moso bamboo forests, increasing the duration of N deposition manipulation is urgent and essential for improving our understanding of the role of canopy processes in ecosystem carbon fluxes in the future.

Supplementary Materials: The following are available online at <https://www.mdpi.com/article/10.3390/f12101427/s1>, Figure S1: The correlations between total soil respiration (RS, a), autotrophic respiration (RA, b), heterotrophic respiration (RH, c) and soil moisture (%) at 5 cm., Table S1: *p* values of one-way analysis of variance for soil temperature and moisture at the depth of 5 cm, Table S2: Coefficients of different models of the relationships between soil respiration ($\mu\text{mol CO}_2 \text{ m}^{-2} \text{ s}^{-1}$) and soil moisture (%) at 5 cm depth.

Author Contributions: All authors contributed to the development of ideas and analysis of output results. C.C., X.T., and S.F. conceived the study; Z.Y., L.L., Y.L., and J.L. performed the research and data acquisition; C.C. and X.T. contributed to the data analysis; X.T. and C.C. wrote the first draft; All authors have read and agreed to the published version of the manuscript.

Funding: This study was primarily supported by National Natural Science Foundation of China (31800365), Fundamental Research Funds for Platform of International Centre for Bamboo and Rattan (1632020003), Operation Funding of Innovation Platform of Forest and Grass Technology (2021132033 and 2021132035), State Key Laboratory of Geohazard Prevention and Geoenvironment Protection Independent Research Project (SKLGP2018Z004), and the Everest Scientific Research Program of Chengdu University of Technology (80000-2021ZF11410).

Institutional Review Board Statement: Not applicable.

Informed Consent Statement: Not applicable.

Data Availability Statement: The data presented in this study are available on request from the corresponding author, Xiaolu Tang.

Conflicts of Interest: The authors declare no conflict of interest.

References

1. Yu, G.; Jia, Y.; He, N.; Zhu, J.; Chen, Z.; Wang, Q.; Piao, S.; Liu, X.; He, H.; Guo, X.; et al. Stabilization of atmospheric nitrogen deposition in China over the past decade. *Nat. Geosci.* **2019**, *12*, 424–429. [\[CrossRef\]](#)
2. Galloway, J.N.; Dentener, F.J.; Capone, D.G.; Boyer, E.W.; Howarth, R.W.; Seitzinger, S.P.; Asner, G.P.; Cleveland, C.C.; Green, P.A.; Holland, E.A.; et al. Nitrogen cycles: Past, present, and future. *Biogeochemistry* **2004**, *70*, 153–226. [\[CrossRef\]](#)
3. Schwede, D.B.; Simpson, D.; Tan, J.; Fu, J.S.; Dentener, F.; Du, E.; deVries, W. Spatial variation of modelled total, dry and wet nitrogen deposition to forests at global scale. *Environ. Pollut.* **2018**, *243*, 1287–1301. [\[CrossRef\]](#) [\[PubMed\]](#)
4. Liu, X.; Zhang, Y.; Han, W.; Tang, A.; Shen, J.; Cui, Z.; Vitousek, P.; Erisman, J.W.; Goulding, K.; Christie, P.; et al. Enhanced nitrogen deposition over China. *Nature* **2013**, *494*, 459. [\[CrossRef\]](#)
5. Ma, S.; Chen, G.; Du, E.; Tian, D.; Xing, A.; Shen, H.; Ji, C.; Zheng, C.; Zhu, J.; Zhu, J.; et al. Effects of nitrogen addition on microbial residues and their contribution to soil organic carbon in China's forests from tropical to boreal zone. *Environ. Pollut.* **2021**, *268*, 115941. [\[CrossRef\]](#) [\[PubMed\]](#)
6. Janssens, I.A.; Dieleman, W.; Luyssaert, S.; Subke, J.A.; Reichstein, M.; Ceulemans, R.; Ciais, P.; Dolman, A.J.; Grace, J.; Matteucci, G.; et al. Reduction of forest soil respiration in response to nitrogen deposition. *Nat. Geosci.* **2010**, *3*, 315–322. [\[CrossRef\]](#)
7. Yu, M.; Wang, Y.P.; Baldock, J.A.; Jiang, J.; Mo, J.; Zhou, G.; Yan, J. Divergent responses of soil organic carbon accumulation to 14 years of nitrogen addition in two typical subtropical forests. *Sci. Total Environ.* **2020**, *707*, 136104. [\[CrossRef\]](#) [\[PubMed\]](#)
8. Xu, X.; Yan, L.; Xia, J. A threefold difference in plant growth response to nitrogen addition between the laboratory and field experiments. *Ecosphere* **2019**, *10*, e02572. [\[CrossRef\]](#)
9. Schulte-Uebbing, L.; de Vries, W. Global-scale impacts of nitrogen deposition on tree carbon sequestration in tropical, temperate, and boreal forests: A meta-analysis. *Glob. Chang. Biol.* **2018**, *24*, e416–e431. [\[CrossRef\]](#)
10. LeBauer, D.S.; Treseder, K.K. Nitrogen limitation of net primary productivity in terrestrial ecosystems is globally distributed. *Ecology* **2008**, *89*, 371–379. [\[CrossRef\]](#)
11. Wang, J.; Song, B.; Ma, F.; Tian, D.; Li, Y.; Yan, T.; Quan, Q.; Zhang, F.; Li, Z.; Wang, B.; et al. Nitrogen addition reduces soil respiration but increases the relative contribution of heterotrophic component in an alpine meadow. *Funct. Ecol.* **2019**, *33*, 2239–2253. [\[CrossRef\]](#)
12. Li, Q.; Song, X.; Chang, S.X.; Peng, C.; Xiao, W.; Zhang, J.; Xiang, W.; Li, Y.; Wang, W. Nitrogen depositions increase soil respiration and decrease temperature sensitivity in a Moso bamboo forest. *Agric. For. Meteorol.* **2019**, *268*, 48–54. [\[CrossRef\]](#)

13. Tremblay, S.L.; D'Orangeville, L.; Lambert, M.-C.; Houle, D. Transplanting boreal soils to a warmer region increases soil heterotrophic respiration as well as its temperature sensitivity. *Soil Biol. Biochem.* **2018**, *116*, 203–212. [\[CrossRef\]](#)
14. Peng, Q.; Dong, Y.; Qi, Y.; Xiao, S.; He, Y.; Ma, T. Effects of nitrogen fertilization on soil respiration in temperate grassland in Inner Mongolia, China. *Environ. Earth Sci.* **2011**, *62*, 1163–1171. [\[CrossRef\]](#)
15. Du, Y.; Guo, P.; Liu, J.; Wang, C.; Yang, N.; Jiao, Z. Different types of nitrogen deposition show variable effects on the soil carbon cycle process of temperate forests. *Glob. Chang. Biol.* **2014**, *20*, 3222–3228. [\[CrossRef\]](#)
16. Gaige, E.; Dail, D.B.; Hollinger, D.Y.; Davidson, E.A.; Fernandez, I.J.; Sievering, H.; White, A.; Halteman, W. Changes in canopy processes following whole-forest canopy nitrogen fertilization of a mature Spruce-Hemlock forest. *Ecosystems* **2007**, *10*, 1133–1147. [\[CrossRef\]](#)
17. Houle, D.; Marty, C.; Duchesne, L. Response of canopy nitrogen uptake to a rapid decrease in bulk nitrate deposition in two eastern Canadian boreal forests. *Oecologia* **2015**, *177*, 29–37. [\[CrossRef\]](#)
18. Lu, X.; Ren, W.; Hou, E.; Zhang, L.; Wen, D.; Liu, Z.; Lin, Y.; Wang, J.; Kuang, Y. Negative effects of canopy N addition on soil organic carbon in wet season are primarily detected in uppermost soils of a subtropical forest. *Global Ecol. Conserv.* **2019**, *17*, e00543. [\[CrossRef\]](#)
19. Zhang, W.; Shen, W.; Zhu, S.; Wan, S.; Luo, Y.; Yan, J.; Wang, K.; Lei, L.; Dai, H.; Li, P. Can canopy addition of nitrogen better illustrate the effect of atmospheric nitrogen deposition on forest ecosystem? *Sci. Rep.* **2015**, *5*, 11245. [\[CrossRef\]](#) [\[PubMed\]](#)
20. Hu, Y.; Zhao, P.; Zhu, L.; Zhao, X.; Ni, G.; Ouyang, L.; Schafer, K.V.R.; Shen, W. Responses of sap flux and intrinsic water use efficiency to canopy and understory nitrogen addition in a temperate broadleaved deciduous forest. *Sci. Total Environ.* **2019**, *648*, 325–336. [\[CrossRef\]](#)
21. Jiang, X.; Liu, N.; Lu, X.; Huang, J.G.; Cheng, J.; Guo, X.; Wu, S. Canopy and understory nitrogen addition increase the xylem tracheid size of dominant broadleaf species in a subtropical forest of China. *Sci. Total Environ.* **2018**, *642*, 733–741. [\[CrossRef\]](#)
22. Chen, H.; Li, D.; Gurmesa, G.A.; Yu, G.; Li, L.; Zhang, W.; Fang, H.; Mo, J. Effects of nitrogen deposition on carbon cycle in terrestrial ecosystems of China: A meta-analysis. *Environ. Pollut.* **2015**, *206*, 352–360. [\[CrossRef\]](#) [\[PubMed\]](#)
23. Wang, C.; Yang, X.; Xu, K. Effect of chronic nitrogen fertilization on soil CO₂ flux in a temperate forest in North China: A 5-year nitrogen addition experiment. *J. Soils Sed.* **2018**, *18*, 506–516. [\[CrossRef\]](#)
24. Nguyen, T.T.; Marschner, P. Soil respiration, microbial biomass and nutrient availability in soil after addition of residues with adjusted N and P concentrations. *Pedosphere* **2017**, *27*, 76–85. [\[CrossRef\]](#)
25. Bae, K.; Fahey, T.J.; Yanai, R.D.; Fisk, M. Soil nitrogen availability affects belowground carbon allocation and soil respiration in northern hardwood forests of New Hampshire. *Ecosystems* **2015**, *18*, 1179–1191. [\[CrossRef\]](#)
26. Tian, J.; Dungait, J.A.J.; Lu, X.; Yang, Y.; Hartley, I.P.; Zhang, W.; Mo, J.; Yu, G.; Zhou, J.; Kuzyakov, Y. Long-term nitrogen addition modifies microbial composition and functions for slow carbon cycling and increased sequestration in tropical forest soil. *Glob. Chang. Biol.* **2019**, *25*, 3267–3281. [\[CrossRef\]](#) [\[PubMed\]](#)
27. Du, H.Q.; Zhou, G.M.; Fan, W.Y.; Ge, H.L.; Xu, X.J.; Shi, Y.J.; Fan, W.L. Spatial heterogeneity and carbon contribution of aboveground biomass of moso bamboo by using geostatistical theory. *Plant Ecol.* **2010**, *207*, 131–139. [\[CrossRef\]](#)
28. Song, X.; Peng, C.; Zhou, G.; Gu, H.; Li, Q.; Zhang, C. Dynamic allocation and transfer of non-structural carbohydrates, a possible mechanism for the explosive growth of Moso bamboo (*Phyllostachys heterocycla*). *Sci. Rep.* **2016**, *6*, 25908. [\[CrossRef\]](#) [\[PubMed\]](#)
29. Tang, X.; Fan, S.; Qi, L.; Guan, F.; Du, M.; Zhang, H. Soil respiration and net ecosystem production in relation to intensive management in Moso bamboo forests. *Catena* **2016**, *137*, 219–228. [\[CrossRef\]](#)
30. Song, X.Z.; Zhou, G.M.; Jiang, H.; Yu, S.Q.; Fu, J.H.; Li, W.Z.; Wang, W.F.; Ma, Z.H.; Peng, C.H. Carbon sequestration by Chinese bamboo forests and their ecological benefits: Assessment of potential, problems, and future challenges. *Environ. Rev.* **2011**, *19*, 418–428. [\[CrossRef\]](#)
31. Jia, Z.; Zhang, J.; Wang, X.; Xu, J.; Li, Z. *Report for Chinese Forest Resource—The 7th National Forest Inventory*; China Forestry Publishing House: Beijing, China, 2009; p. 60. (In Chinese)
32. Li, Y.; Feng, P. Bamboo resources in China based on the ninth national forest inventory data. *World Bamboo Ratt.* **2019**, *17*, 45–48, (In Chinese with English Abstract).
33. Song, X.; Chen, X.; Zhou, G.; Jiang, H.; Peng, C. Observed high and persistent carbon uptake by Moso bamboo forests and its response to environmental drivers. *Agric. For. Meteorol.* **2017**, *247*, 467–475. [\[CrossRef\]](#)
34. Zhang, J.; Li, Q.; Lv, J.; Peng, C.; Gu, Z.; Qi, L.; Song, X.; Song, X. Management scheme influence and nitrogen addition effects on soil CO₂, CH₄, and N₂O fluxes in a Moso bamboo plantation. *For. Ecosyst.* **2021**, *8*, 6. [\[CrossRef\]](#)
35. Gao, Q.; Dai, B.; Luo, C.; Liu, L.; Ma, D.; Zhang, C. Spatial heterogeneity of soil physical properties in *Phyllostachys heterocycla cv pubescens* forest, South Sichuan Bamboo Sea. *Acta Ecol. Sin.* **2016**, *36*, 2255–2263, (In Chinese with English Abstract).
36. Tian, H.; Yang, J.; Lu, C.; Xu, R.; Canadell, J.G.; Jackson, R.B.; Arneeth, A.; Chang, J.; Chen, G.; Ciais, P.; et al. The Global N₂O Model Intercomparison Project. *Bull. Am. Meteorol. Soc.* **2018**, *99*, 1231–1251. [\[CrossRef\]](#)
37. Tang, X.; Fan, S.; Qi, L.; Guan, F.; Su, W.; Du, M. A comparison of soil respiration, carbon balance and root carbon use efficiency in two managed Moso bamboo forests in subtropical China. *Ann. For. Res.* **2016**, *59*, 3–20. [\[CrossRef\]](#)
38. Subke, J.-A.; Inglima, I.; Francesca Cotrufo, M. Trends and methodological impacts in soil CO₂ efflux partitioning: A metaanalytical review. *Glob. Chang. Biol.* **2006**, *12*, 921–943. [\[CrossRef\]](#)
39. Tang, X.; Fan, S.; Qi, L.; Guan, F.; Cai, C.; Du, M. Soil respiration and carbon balance in a Moso bamboo (*Phyllostachys heterocycla* (Carr.) Mitford cv. *Pubescens*) forest in subtropical China. *IForest-Biogeosciences For.* **2015**, *8*, 606–614. [\[CrossRef\]](#)

40. Jian, J.; Steele, M.K.; Day, S.D.; Quinn Thomas, R.; Hodges, S.C. Measurement strategies to account for soil respiration temporal heterogeneity across diverse regions. *Soil Biol. Biochem.* **2018**, *125*, 167–177. [\[CrossRef\]](#)
41. Zhang, H.X.; Zhuang, S.Y.; Sun, B.; Ji, H.B.; Li, C.M.; Zhou, S. Estimation of biomass and carbon storage of moso bamboo (*Phyllostachys pubescens* Mazel ex Houz.) in southern China using a diameter-age bivariate distribution model. *Forestry* **2014**, *87*, 674–682. [\[CrossRef\]](#)
42. Zhou, G.; Jiang, P.; Xu, Q. (Eds.) *Carbon Sequestration and Transform in Bamboo Ecosystem*; Science Press: Beijing, China, 2010; pp. 105–137. (In Chinese)
43. Zhou, G.; Jiang, P. Density, storage and spatial distributbion of carbon in *Phyllostachy pubescens* forest. *Sci. Silvae Sin.* **2004**, *40*, 20–24, (In Chinese with English Abstract).
44. Tang, X.; Fan, S.; Qi, L.; Guan, F.; Liu, G.; Du, M. Effects of understory removal on root production, turnover and total belowground carbon allocation in Moso bamboo forests. *IForest* **2016**, *9*, 187–194. [\[CrossRef\]](#)
45. Brunner, I.; Bakker, M.R.; Björk, R.G.; Hirano, Y.; Lukac, M.; Aranda, X.; Børja, I.; Eldhuset, T.D.; Helmisaari, H.S.; Jourdan, C.; et al. Fine-root turnover rates of European forests revisited: An analysis of data from sequential coring and ingrowth cores. *Plant Soil* **2013**, *362*, 357–372. [\[CrossRef\]](#)
46. McClaugherty, C.A.; Aber, J.D.; Melillo, J.M. The role of fine roots in the organic matter and nitrogen budgets of two forested ecosystems. *Ecology* **1982**, *63*, 1481–1490. [\[CrossRef\]](#)
47. Tang, X.; Fan, S.; Qi, L.; Liu, G.; Guan, F.; Du, M.; Shen, C. Effect of different managements on carbon storage and carbon allocation in Moso Bamboo Forest (*Phyllostachys pubescen*). *Acta Agric. Univ. Jiangxiensis* **2012**, *34*, 736–742, (In Chinese with English abstract).
48. R Core Team. *R: A Language and Environment for Statistical Computing*; R Foundation for Statistical Computing: Vienna, Austria, 2019; Available online: <http://www.R-project.org/> (accessed on 11 June 2019).
49. Lloyd, J.; Taylor, J. On the temperature dependence of soil respiration. *Funct. Ecol.* **1994**, *8*, 315–323. [\[CrossRef\]](#)
50. Yuste, J.C.; Janssens, I.A.; Carrara, A.; Meiresonne, L.; Ceulemans, R. Interactive effects of temperature and precipitation on soil respiration in a temperate maritime pine forest. *Tree Phys.* **2003**, *23*, 1263–1270. [\[CrossRef\]](#) [\[PubMed\]](#)
51. Lee, M.S.; Nakane, K.; Nakatsubo, T.; Koizumi, H. Seasonal changes in the contribution of root respiration to total soil respiration in a cool-temperate deciduous forest. *Plant Soil* **2003**, *255*, 311–318. [\[CrossRef\]](#)
52. Fan, S.; Xiao, F.; Wang, S.; Guan, F.; Yu, X.; Shen, Z. Soil respiration of Moso bamboo plantation in Huitong, Hu’nan Province. *Acta Eco. Sin.* **2009**, *29*, 5971–5977, (In Chinese with English Abstract).
53. Song, X.; Yuan, H.; Kimberley, M.O.; Jiang, H.; Zhou, G.; Wang, H. Soil CO₂ flux dynamics in the two main plantation forest types in subtropical China. *Sci. Total Environ.* **2013**, *444*, 363–368. [\[CrossRef\]](#)
54. Liu, J.; Jiang, P.; Wang, H.; Zhou, G.; Wu, J.; Yang, F.; Qian, X. Seasonal soil CO₂ efflux dynamics after land use change from a natural forest to Moso bamboo plantations in subtropical China. *For. Ecol. Manag.* **2011**, *262*, 1131–1137. [\[CrossRef\]](#)
55. Wang, C.; Yang, Z.J.; Chen, G.S.; Fan, Y.X.; Liu, Q.; Tian, H. Characteristics of soil respiration in *Phyllostachys edulis* forest in Wanmulin Natural Reserve and related affecting factors. *Chin. J. App. Eco* **2011**, *22*, 1212–1218. (In Chinese)
56. Wang, W.; Chen, W.; Wang, S. Forest soil respiration and its heterotrophic and autotrophic components: Global patterns and responses to temperature and precipitation. *Soil Biol. Biochem.* **2010**, *42*, 1236–1244.
57. Tu, L.H.; Hu, T.X.; Zhang, J.; Li, X.W.; Hu, H.L.; Liu, L.; Xiao, Y.L. Nitrogen addition stimulates different components of soil respiration in a subtropical bamboo ecosystem. *Soil Biol. Biochem.* **2013**, *58*, 255–264. [\[CrossRef\]](#)
58. Song, X.Z.; Peng, C.H.; Zhao, Z.Y.; Zhang, Z.T.; Guo, B.H.; Wang, W.F.; Jiang, H.; Zhu, Q.A. Quantification of soil respiration in forest ecosystems across China. *Atmos. Environ.* **2014**, *94*, 546–551. [\[CrossRef\]](#)
59. Hanson, P.J.; Edwards, N.T.; Garten, C.T.; Andrews, J.A. Separating root and soil microbial contributions to soil respiration: A review of methods and observations. *Biogeochemistry* **2000**, *48*, 115–146. [\[CrossRef\]](#)
60. Kuzyakov, Y. Sources of CO₂ efflux from soil and review of partitioning methods. *Soil Biol. Biochem.* **2006**, *38*, 425–448. [\[CrossRef\]](#)
61. Bond-Lamberty, B.; Bailey, V.L.; Chen, M.; Gough, C.M.; Vargas, R. Globally rising soil heterotrophic respiration over recent decades. *Nature* **2018**, *560*, 80–83. [\[CrossRef\]](#)
62. Yang, Y.S.; Chen, G.S.; Guo, J.F.; Xie, J.S.; Wang, X.G. Soil respiration and carbon balance in a subtropical native forest and two managed plantations. *Plant Ecol.* **2007**, *193*, 71–84. [\[CrossRef\]](#)
63. Zhang, Y.P.; Tan, Z.H.; Song, Q.H.; Yu, G.R.; Sun, X.M. Respiration controls the unexpected seasonal pattern of carbon flux in an Asian tropical rain forest. *Atmos. Environ.* **2010**, *44*, 3886–3893. [\[CrossRef\]](#)
64. Chen, Z.; Yu, G.; Wang, Q. Magnitude, pattern and controls of carbon flux and carbon use efficiency in China’s typical forests. *Global Planet. Change* **2019**, *172*, 464–473. [\[CrossRef\]](#)
65. Fernandez-Martinez, M.; Vicca, S.; Janssens, I.A.; Luyssaert, S.; Campioli, M.; Sardans, J.; Estiarte, M.; Penuelas, J. Spatial variability and controls over biomass stocks, carbon fluxes, and resource-use efficiencies across forest ecosystems. *Trees—Struct. Funct.* **2014**, *28*, 597–611. [\[CrossRef\]](#)
66. Xiao, F.; Fan, S.; Wang, S.; Guan, F.; Yu, X.; Shen, Z. Estimation of carbon balance in Moso bamboo forest and Chinese fir plantation ecosystem. *Sci. Silvae Sin.* **2010**, *46*, 59–65, (In Chinese with English Abstract).
67. Malhi, Y.; Baldocchi, D.D.; Jarvis, P.G. The carbon balance of tropical, temperate and boreal forests. *Plant Cell Environ.* **1999**, *22*, 715–740. [\[CrossRef\]](#)

-
68. Nave, L.E.; Vogel, C.S.; Gough, C.M.; Curtis, P.S. Contribution of atmospheric nitrogen deposition to net primary productivity in a northern hardwood forest. *Can. J. For. Res.* **2009**, *39*, 1108–1118. [[CrossRef](#)]
 69. Adriaenssens, S.; Staelens, J.; Wuyts, K.; Samson, R.; Verheyen, K.; Boeckx, P. Retention of Dissolved Inorganic Nitrogen by Foliage and Twigs of Four Temperate Tree Species. *Ecosystems* **2012**, *15*, 1093–1107. [[CrossRef](#)]
 70. Tu, L.H.; Chen, G.; Peng, Y.; Hu, H.L.; Hu, T.X.; Zhang, J.; Li, X.W.; Liu, L.; Tang, Y. Soil biochemical responses to nitrogen addition in a bamboo forest. *PLoS ONE* **2014**, *9*, e102315. [[CrossRef](#)] [[PubMed](#)]
 71. Shi, L.; Zhang, H.; Liu, T.; Zhang, W.; Shao, Y.; Ha, D.; Li, Y.; Zhang, C.; Cai, X.-a.; Rao, X.; et al. Consistent effects of canopy vs. understory nitrogen addition on the soil exchangeable cations and microbial community in two contrasting forests. *Sci. Total Environ.* **2016**, *553*, 349–357. [[CrossRef](#)] [[PubMed](#)]
 72. Sparks, J.P. Ecological ramifications of the direct foliar uptake of nitrogen. *Oecologia* **2009**, *159*, 1–13. [[CrossRef](#)]
 73. Bardgett, R.D.; Wardle, D.A. *Aboveground-Belowground Linkages: Biotic Interactions, Ecosystem Processes, and Global Change*; Oxford University Press: Oxford, UK, 2011.
 74. Kuzyakov, Y. Review: Factors affecting rhizosphere priming effects. *J. Plant Nutr. Soil Sci.* **2002**, *165*, 382–396. [[CrossRef](#)]
 75. Hopkins, F.; Gonzalez-Meler, M.A.; Flower, C.E.; Lynch, D.J.; Czimczik, C.; Tang, J.; Subke, J.-A. Ecosystem-level controls on root-rhizosphere respiration. *New Phytol.* **2013**, *199*, 339–351. [[CrossRef](#)] [[PubMed](#)]
 76. Frey, S.D.; Ollinger, S.; Nadelhoffer, K.; Bowden, R.; Brzostek, E.; Burton, A.; Caldwell, B.A.; Crow, S.; Goodale, C.L.; Grandy, A.S.; et al. Chronic nitrogen additions suppress decomposition and sequester soil carbon in temperate forests. *Biogeochemistry* **2014**, *121*, 305–316. [[CrossRef](#)]